Properties of two interlinked $\chi^{(2)}$ interactions in noncollinear phase matching

Maria Bondani

Istituto Nazionale per la Fisica della Materia, Unità di Como, via Valleggio 11, Como 22100, Italy

Alessia Allevi, Emiliano Puddu, and Alessandra Andreoni

Dipartimento di Scienze Chimiche, Fisiche, Matematiche, Università dell'Insubria, via Valleggio 11, Como 22100, Italy, and Istituto Nazionale per la Fisica della Materia, Unità di Como, via Valleggio 11, Como 22100, Italy

Alessandro Ferraro

Dipartimento di Fisica and Istituto Nazionale per la Fisica della Materia, Università di Milano, via Celoria 16, Milano 20133, Italy

Matteo G. A. Paris

Istituto Nazionale per la Fisica della Materia, Unità di Pavia, via Bassi 6, Pavia 27100, Italy

Received June 20, 2003

We present a compact experimental realization of the interaction among five field modes in a $\chi^{(2)}$ nonlinear crystal. The classical evolution of the fields can be analytically described assuming that two of the fields play the role of nondepleted pumps. A peculiar behavior appears that has been experimentally verified. If one of the fields has a nonzero input amplitude, then the other two fields at the output are holographic replicas of the input signal. © 2004 Optical Society of America

OCIS codes: 190.0190, 190.4410, 270.0270, 090.0090.

Multiple nonlinear processes involving several modes of radiation have become essential for achieving all-optical processing[1] and for generation of nonclassical states of light.[2] Systems of this kind need simultaneous phase matching of different interactions, which can be achieved by use of periodically and aperiodically poled crystals with quasi-phase-matching conditions,[3] by use of self-phase-locked parametric oscillators,[4] or, more directly, by implementing a noncollinear phase-matching geometry. In this Letter we present an experimental realization of five-field second-order interactions simultaneously phase matched in a single crystal in the noncollinear interaction geometry depicted in Fig. 1. The focus of the present Letter will be the classical evolution of the system. We refer to Ref. 5 for a quantum description of our scheme. Here we note only that in phase-matching conditions and within the parametric approximation the system is suitable for generating three-mode entangled states, either starting from the vacuum or by seeding the crystal.

In our scheme the interacting fields are provided by the harmonics of a Q-switched amplified Nd:YAG laser (7-ns pulse duration) at wavelengths of $\lambda_1 = \lambda_3 = 1064$ nm, $\lambda_4 = \lambda_5 = 532$ nm (pumps), and $\lambda_2 = 355$ nm. The energy-matching and phase-matching conditions required by the interactions are $\omega_4 = \omega_1 + \omega_3$, $\omega_2 = \omega_3 + \omega_5$, $\mathbf{k}_4 = \mathbf{k}_1 + \mathbf{k}_3$, and $\mathbf{k}_2 = \mathbf{k}_3 + \mathbf{k}_5$, where $\mathbf{k}_j$ are the wave vectors (in the medium) corresponding to ω_j and making angles ϑ_j with the normal to the entrance face of the crystal. It is possible to satisfy these phase-matching conditions with a number of different sets of frequencies and interaction angles depending on the choice of the nonlinear medium. In this Letter we choose a compact interaction geometry in which both the interactions are type I and occur in the noncollinear phase-matching condition. The two pump fields are superimposed in a single beam with mixed polarization (see Fig. 1). The nonlinear crystal was a β-BaB_2O_4 (BBO, cut angle 32°, cross section 10 mm × 10 mm, and thickness 4 mm) and the interaction angles, calculated assuming that $\mathbf{k}_4$ and $\mathbf{k}_5$ were normal to the crystal entrance face, were $\vartheta' = 37.74°$, $\vartheta_1 = -\vartheta_3 = 10.6°$, and $\vartheta_2 = 3.5°$. Since our BBO crystal was cut at 32°, it had to be rotated to allow phase matching, the only consequence of which was reducing the effective aperture of the crystal. The system dynamics can be effectively described by a set of collinear equations.[6] Assuming parametric behavior for modes a_4 and a_5 and perfect phase matching for both interactions, the complex field amplitudes a_j,[7] $j = 1, 2, 3$, obey

$$\mathrm{d}a_1/\mathrm{d}z = -ig_1 a_3^{*}, \qquad \mathrm{d}a_2/\mathrm{d}z = -ig_2 a_3,$$

$$\mathrm{d}a_3/\mathrm{d}z = -ig_1 a_1^{*} - ig_2^{*} a_2, \tag{1}$$

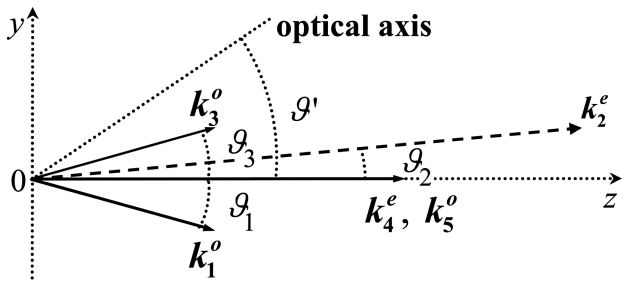

Fig. 1. Schematic diagram of the interaction scheme.

0146-9592/04/020180-03$15.00/0 © 2004 Optical Society of America

where the coupling constants g_1 and g_2 are proportional to the pump amplitudes $a_4(0)$ and $a_5(0)$, respectively.[8] The solutions of Eqs. (1) read as follows:

$$
\begin{aligned}
a_1(z) &= -\frac{1}{\Gamma^2}[|g_1|^2\cos(\Gamma z) - |g_2|^2]a_1(0) \\
&\quad - \frac{g_1 g_2}{\Gamma^2}[\cos(\Gamma z) - 1]a_2{}^*(0) \\
&\quad + \frac{g_1}{\Gamma}\sin(\Gamma z)a_3{}^*(0)\,, \\
a_2(z) &= \frac{g_1 g_2}{\Gamma^2}[\cos(\Gamma z) - 1]a_1{}^*(0) \\
&\quad - \frac{1}{\Gamma^2}[|g_1|^2 - |g_2|^2\cos(\Gamma z)]a_2(0) \\
&\quad - \frac{g_2}{\Gamma}\sin(\Gamma z)a_3(0)\,, \\
a_3(z) &= \frac{g_1{}^*}{\Gamma}\sin(\Gamma z)a_1{}^*(0) + \frac{g_2}{\Gamma}\sin(\Gamma z)a_2(0) \\
&\quad + \cos(\Gamma z)a_3(0)\,, \qquad (2)
\end{aligned}
$$

where $\Gamma = (|g_2|^2 - |g_1|^2)^{1/2}$. The field energies are given by $E_j = \hbar\omega_j|a_j(z)|^2 \times$ (pulse duration) $\times$ (beam cross size). Note that Eqs. (2) describe the fields' evolution for both real and imaginary values of Γ, i.e., both in the oscillatory and in the amplification regimes. The experiments that follow are aimed at checking the phase and intensity properties of these fields.

According to Eqs. (2), if only one of the evolving fields is nonvanishing at the crystal entrance (single seed field), then the two generated fields are holographic replicas of the seed. For $a_1(0) \neq 0$, $a_2(0) = 0$, and $a_3(0) = 0$, both the generated fields are phase conjugate with respect to $a_1(0)$, i.e., $a_2(z) \propto a_1{}^*(0)$ and $a_3(z) \propto a_1{}^*(0)$. We can thus consider the seed field as an object field at ω_1 and expect that fields $a_2(z)$ and $a_3(z)$ reconstruct two real holographic images.

To verify this behavior, we adopted the experimental setup shown in Fig. 2, where the two pumps are provided by the second-harmonic field from the laser, which is elliptically polarized. As the object O, we inserted a regular plastic net (80-μm-diameter wires spaced 120 μm apart) into the beam at ω_1 at a distance $d = 20$ cm from the BBO crystal. In this way the field diffracted by the net entirely covered the BBO crystal. In Figs. 2(b) and 2(c) we show holographic images of the net as detected by a CCD camera along the direction of the output fields at ω_3 at a distance $d \simeq 20.5$ cm [Fig. 2(b)] and at ω_2 at a distance $3d \simeq 58$ cm [Fig. 2(c)]. The distances fit those that are expected,[8] and the transverse dimensions are the same as those of the original object, again in good agreement with theory.[9]

As a further check of Eqs. (2) we performed two different experiments in which the interactions were seeded by either field a_1 (case 1) or field a_2 (case 2). The experimental setups are shown in Fig. 3. The relevant harmonic outputs of the laser were sent to harmonic separators. We separated the two polarization components of the second harmonics with a thin-film plate polarizer (P_1 in Fig. 3) and inserted a $\lambda/2$ plate into the ordinarily polarized component to obtain a variable pump, a_5, without affecting the other pump, a_4. The two pump fields were then recombined through a second thin-film plate polarizer (P_2) and sent to the BBO crystal. The diameters of the beams were ~6 mm, thus ensuring overlap inside the crystal. In case 1 the seed field at ω_1 was a fraction of the residual fundamental from the laser.

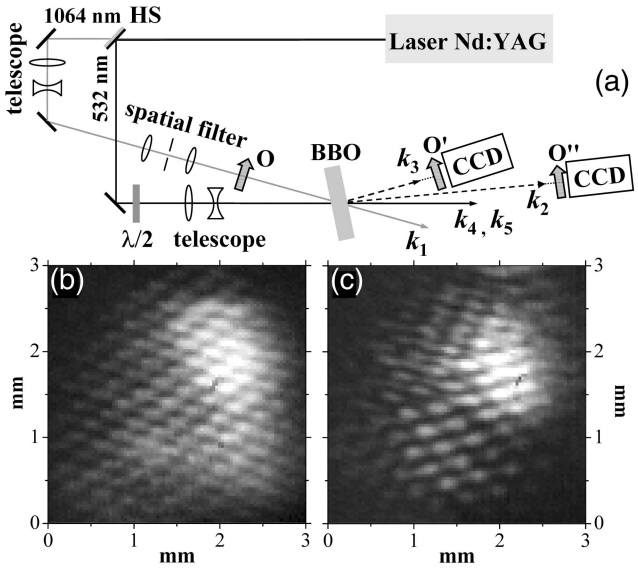

Fig. 2. (a) Experimental setup for verification of the holographic properties of the generated fields. HS, harmonic separator; O, object; O′ and O″, the reconstructed real holographic images at ω_3 and ω_2, respectively. (b) Holographic image at ω_3. (c) Holographic image at ω_2.

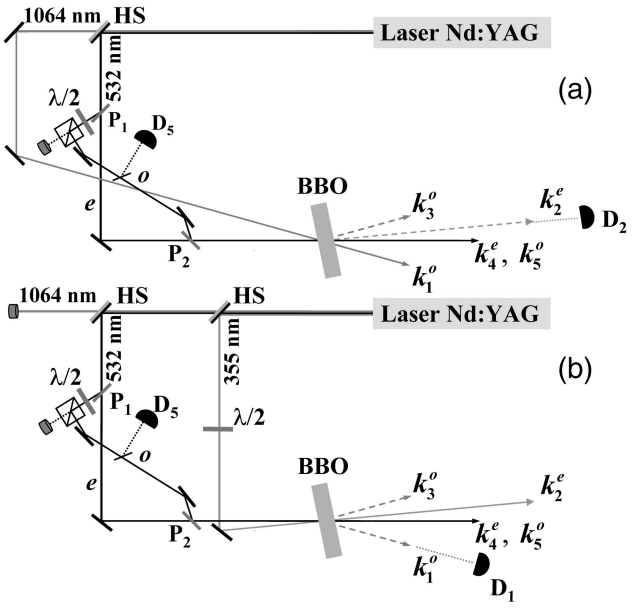

Fig. 3. Schemes of the experimental setups in (a) case 1 and (b) case 2. $\lambda/2$, half-wave plate; P_j, thin-film plate polarizers; D_j, energy detectors.

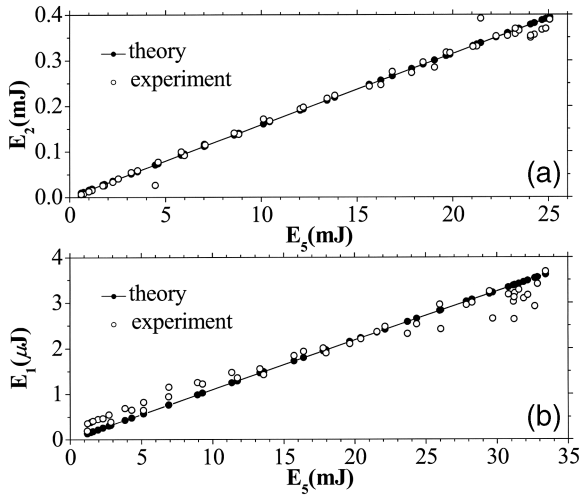

Fig. 4. (a) Measured (open circles) and calculated [from Eq. (3), filled circles] energy at ω_2 (case 1, see text) as a function of the measured energy of the pump at ω_5. (b) Same as (a) but for case 2 (see text).

This field was polarized at 45°, such that ~50% of its photons were useful for the interaction. In case 2 the polarization of the seed field at ω_2 (third harmonics) had to be optimally rotated by a $\lambda/2$ plate. The pump and seed fields were measured by pyroelectric detectors as averages over more than 100 pulses. Pump energy E_4 was measured with an ED500 detector (Gentec Electro-Optics, Inc.) inserted after P_2 in both cases 1 and 2. The measured values were $E_4 = 158$ mJ/pulse in case 1 and $E_4 = 68$ mJ/pulse in case 2. As for the energies of the seeding fields, we found, in case 1, $E_1 = 48$ mJ/pulse, as measured with a Gentec Electro-Optics ED200 detector (useful $E_1 = 24$ mJ), and in case 2, $E_2 = 3.5$ mJ/pulse, as found by use of a PE10 detector (Ophir Optronics, Ltd.). To obtain a reliable measurement of energy E_5, we inserted a polarizing cube beam splitter and a calibrated glass plate to extract a fraction of the field (see Fig. 3). The variation of E_5 was achieved by rotation of the $\lambda/2$ plate, and the measurement of the energy was performed in case 1 with the ED500 detector, and in case 2 with the PE10 detector (see D_5 in Fig. 3). Finally, we measured energy E_2, in case 1, with a PE10 detector (see D_2 in Fig. 3). The values of E_5 and E_2 were measured simultaneously as averages over the same 20 laser shots at each rotation of the $\lambda/2$ plate and for fixed values of energies E_4 and E_1. The experimental values are shown in Fig. 4(a) as open circles. To compare the measured values with the theoretical predictions we plot in the same figure (filled circles) the values of E_2 as calculated from Eqs. (2) for the same experimental values of E_5, E_4, and E_1, i.e.,

$$E_2 = \frac{\omega_2}{\omega_1} \frac{E_1 \alpha E_4 \beta E_5 \{\cos[(\beta E_5 - \alpha E_4)^{1/2} z] - 1\}^2}{(\beta E_5 - \alpha E_4)^2}, \quad (3)$$

where $\alpha = 8.3 \times 10^4$ $(\mathrm{J\,m^2})^{-1}$ and $\beta = 2.6 \times 10^5$ $(\mathrm{J\,m^2})^{-1}$ are coefficients that include the coupling constants and the conversion from photon fluxes to energies. The agreement between measured and calculated values is excellent. The validity of the parametric approximation can also be checked by comparison of the relative scale of E_2 with those of E_4 and E_5. In case 2, energy E_1 of the field generated at ω_1 was too low to be measured with a pyroelectric detector, and we thus used a calibrated CCD camera (Pulnix Model PE2015). The values of E_5 and E_1 were again measured simultaneously and averaged over the same 20 laser shots while energies E_4 and E_2 were kept fixed. The experimental values are shown in Fig. 4(b) as open circles. The theoretical expression shown in the same figure as filled circles is calculated for the experimental values of E_5, E_4, and E_2 from Eq. (3) by interchanging subscripts 1 and 2. The agreement between measured and calculated values is good, although not as in the previous case, because of the lower energy values involved in the interaction.

This work was partially supported by Istituto Nazionale per la Fisica della Materia project PRA-2002-CLON. The authors thank F. Paleari (Università dell'Insubria) for valuable experimental suggestions. M. Bondani's e-mail address is maria.bondani@uninsubria.it.

References

1. T. Kartaloğlu, Z. G. Figen, and O. Aytür, J. Opt. Soc. Am. **20,** 343 (2003), and references therein.
2. J. Zhang, C. Xie, and K. Peng, Phys. Rev. A **66,** 032318 (2002).
3. R. L. Byer, J. Nonlinear Opt. Phys. Mater. **6,** 549 (1997).
4. J.-J. Zondy, A. Douillet, A. Tallet, E. Ressayre, and M. Le Berre, Phys. Rev. A **63,** 023814 (2001).
5. A. Ferraro, M. G. A. Paris, A. Allevi, A. Andreoni, M. Bondani, and E. Puddu, *arXiv.org e-Print archive*, quant-ph/0306109, June 16, 2003, http://arXiv.org/abs/quant-ph/0306109.
6. A fully noncollinear analytical solution of the system can be found. For the experimental parameters in this Letter the differences with the collinear solution are minimal.
7. B. E. A. Saleh and C. M. Tech, *Fundamentals of Photonics* (Wiley, New York, 1991), p. 764.
8. M. Bondani and A. Andreoni, Phys. Rev. A **66,** 033805 (2002).
9. M. Bondani, A. Allevi, and A. Andreoni, J. Opt. Soc. Am. B **20,** 1 (2003).